THE COMPENSATION MECHANISM OF CERVICAL MUSCLE DYSFUNCTION ON SPINAL STABILITY – AN IN VITRO STUDY USING PORCINE MODEL

Chih-Hsiu Cheng, Pei-Jing Chen, Ya-Wen Kuo, and Jaw-Lin Wang*

ABSTRACT

Muscle injury/impairment results in decreased muscle forces. Decreased muscle forces can be compensated by synergic muscle forces. However, the effects of muscle dysfunction and compensation on spinal stability are not clear yet. Eight porcine cervical spine specimens (C2-T1) were tested by the spine flexibility testing apparatus. The apparatus was equipped with muscle force replication of three paired cervical muscles. The simulations of muscle recruitment included; no muscle recruitment, normal muscle recruitment, muscle dysfunction without compensation, and muscle dysfunction with two compensation strategies: the minimized muscle forces and the minimized axial forces. The spinal stability was examined by the neutral zone (NZ) and range of motion (ROM), which was the sagittal motion of specimen applied with external moment at 0.5 and 2 Nm respectively. Initial positions of specimens were also recorded. NZ and ROM were largest in the no muscle test, and smallest in the muscle dysfunction without compensation test. NZ and ROM of muscle dysfunction with minimal axial force compensation were larger than those with minimal muscle force compensation. This study concluded that: (1) the muscle dysfunction without compensation constrains spinal motion; (2) impaired muscle with compensations cannot stabilize cervical spine efficiently as normal muscles does; and (3) compensation strategy of minimal muscle forces provides better spinal stability than that of minimal axial forces.

Key Words: cervical spine, stability, muscle force, muscle dysfunction.

I. INTRODUCTION

An unstable spine is clinically defined as the state of excessive spinal motion beyond the normal physiological limits (Nachemson, 1985). Muscles are important in maintaining the spinal stability by increasing the bending stiffness (Essendrop *et al.*, 2002; Lee *et al.*, 2006). Muscular disorders from repetitive work or strain injuries in the neck region distort muscle responses (Andersen *et al.*, 2007). Impaired muscles usually show decreased muscle force, and can be compensated for by intact synergic muscles (Edgerton *et al.*, 1996). The effect of compensation for impaired muscles on spinal stability is, however, less understood.

The issues of spinal stability controlled by the active muscular system are complicated since the numbers of muscles surrounding the spinal segments are larger than the degrees of freedom of the musculoskeletal system. Previous studies examined the relationship between muscle forces and spinal stability by the biomechanical models (Crisco *et al.*, 1991; Snijders *et al.*, 1991) or the EMG-driven models (Hughes *et al.*, 1994; Langenderfer *et al.*, 2005). Since the musculoskeletal system is static/dynamic indeterminate, the numerical optimization method is frequently used in those models to solve indeterminate problems of the musculoskeletal system (Choi *et al.*, 1999; Moroney *et al.*, 1988). The non-linear cost functions such as sum of square muscle forces or sum of square spinal loads are used to minimize the consumed energy or to minimize the compressive stress on the intervertebral disc respectively. The

*Corresponding author. (Tel: 886-2-33665269; Fax: 886-2-23687573; Email: jlwang@ntu.edu.tw)
The authors are with the Institute of Biomedical Engineering, National Taiwan University, Taiwan, R.O.C.

optimizations subject to those cost functions are commonly presumed to comply with the control strategy of the central nerve system (CNS) (Arjmand *et al.*, 2006; Brown *et al.*, 2005; Buchanan *et al.*, 1996).

Previous in vitro studies showed the feasibility of using mechanical muscle simulations to study the spinal stability (Panjabi *et al.*, 1989; Wilke *et al.*, 1995). Kettler *et al.* (2002) focused on the cervical muscle forces and showed that the simulation of six cervical muscles strongly stabilizes the intact or injured upper cervical spine specimens. Nevertheless, the muscle dysfunction and compensation conditions have been less addressed in the in vitro studies.

This in vitro study used porcine spine models to investigate the mechanism of muscle compensation strategies of impaired muscle on the cervical spine stability. The optimization method of minimal muscle force and minimal axial force was used to derive the muscle forces. The results of this study may help to clarify: 1) the effect of impaired muscles on spinal stability; 2) the effect of impaired muscles with compensation strategy on spinal stability; and 3) which compensation strategy provides better spinal stability.

II. MATERIALS & METHODS

1. Testing Apparatus

The spine flexibility testing apparatus, which comprised a frame construct, a force replication system and a motion acquisition system, was used (Fig 1). The force replication system can generate external pure moments and simulate muscle forces on the specimen. It included a jig with two parallel plates. Two cables were attached to each plate to generate pure moment, and six cables were attached to the jig to simulate the muscle forces. The jig was to clamp the cranial part of the specimen. The weight of the jig was counter balanced throughout the test by a weight hung over the traveling pulley. The two cables of each plate were pulled through sideways pulleys with equal weight pulling in the opposite direction. A total of four cables on the parallel plates produced two equal force couples to create pure moment. The fine tune tackles were used to adjust the height of sideways pulleys to keep the tangential forces from the four cables horizontally. The adjustment ensured the applied moments were constant during the deformation of the spine specimen (Panjabi, 2007).

The muscle pairs of the current study included symmetrical neck flexors (sternocleidomastoid, SCM) and extensors (splenius capitis, SPL; semispinalis capitis, SSC), which are the main cervical muscles in maintaining the neck dynamic stability (Vasavada *et al.*, 1998). Each muscle force was generated by a given weight so as to keep it a constant force during the whole test session. The orientation of each muscle, which was defined by the origin and insertion of the major muscle bands, was determined using the results of a previous study (Vasavada *et al.*, 1998) (Fig. 2). The resultant forces on the specimens were measured by an S-type load cell (STC-50kgSE, Vishay, USA) placed below the specimen.

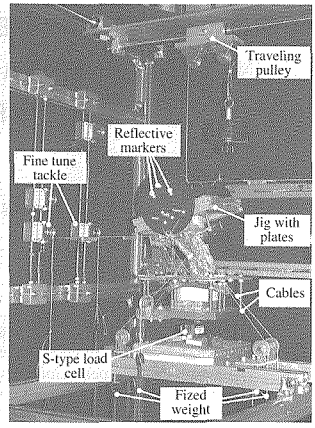

Fig. 1 Spinal muscle replication system

A two-camera stereophotogrammetric analysis system was used to determine the three-dimensional motion of the specimen. Three reflective markers were placed on the jig for the measurement of motion. The direct linear transformation method was used to transform the 2D images into rotational angles of three axes. The angular resolution of the motion acquisition system is higher than 0.2° over the range of -90°~90° verified by absolute angles from an index plate. The motion acquisition system was calibrated before each testing.

2. Specimen Preparation

Eight cervical spines (C2-T1, length: 14.9 ± 0.8 cm) from 6 month-old swine were used. The muscular tissues of specimens were removed and the specimens were frozen at -20°C for storage. The specimens were moved to a refrigerator (4°C) one night before testing and were thawed at room temperature for five hours before testing. The cranial and caudal vertebrae were potted with polymethylmethacrylate. The cranial part of the specimen was clamped by the jig, and the caudal part was fixed on the mounting table of the frame. During the experiment, the specimens were moisturized with saline-soaked gauze.

Table 1 Magnitude of muscle forces (unit: N) in different muscle recruitment tests

	SCM_R	SCM_L	SPL_R	SPL_L	SSC_R	SSC_L
Normal muscle recruitment	18	18	13	13	17	17
SCM dysfunction without compensation	4	18	13	13	17	17
SCM dysfunction with minimal muscle force compensation	4	4	1	1	18	18
SCM dysfunction with minimal axial force compensation	4	3	0	1	35	1

Subscripts "*R*" and "*L*" indicate the right and left side muscle respectively.

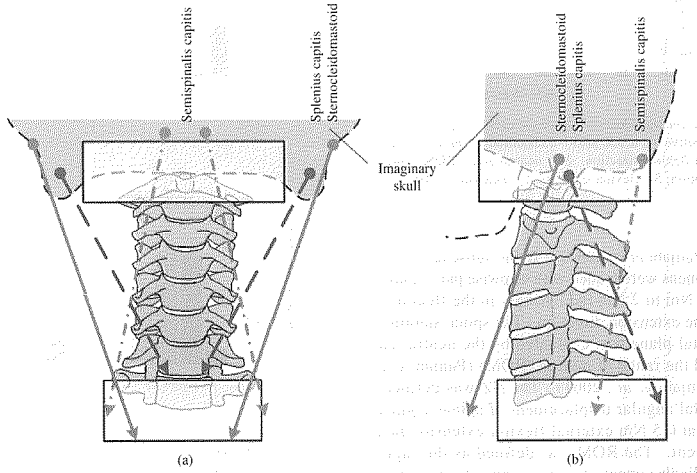

Fig. 2 Schematic plot for the arrangement of the muscles on the specimen. (a) coronal view; (b) sagittal view.

3. Experimental Procedure and Measurement

The experiment included the following five muscle recruitment conditions: 1) no muscle recruitment; 2) normal muscle recruitment; 3) right side SCM dysfunction without compensation; 4) right side SCM dysfunction with minimal muscle force compensation strategy; and 5) right side SCM dysfunction with minimal axial force compensation strategy. The muscle forces in normal muscle recruitment test were calculated by the following conditions: 1) the net moments of three axes were zero; 2) the resultant shear force in lateral direction was zero; 3) the resultant axial force was 85 N (Snijders *et al.*, 1991); and 4) the summation of square muscle forces was minimum. The muscle force of impaired SCM was set to be 4 N, about 1/4 of that in normal muscle recruitment test. Then the other muscle forces in right side SCM dysfunction with minimal muscle force compensation test were derived from the following conditions: 1) the net moments of three axes were zero; 2) the resultant shear force in anteroposterior direction was the same as that in normal muscle recruitment test; and 3) the summation of square muscle forces was minimum. The other muscle forces in right side SCM dysfunction with minimal axial force compensation test were derived from the same first two conditions as those in SCM dysfunction with minimal muscle force compensation test, and the cost function was changed to be: the summation of square axial forces. The first two conditions for the two compensation strategies were to minimize the changes of initial position in compensation tests from that in normal muscle recruitment test, and the cost functions were to minimize energy expenditure and compressive stress respectively. The summary of the muscle forces is shown in Table 1.

In the beginning of each test, the initial positions in three planes and the resultant axial force at C7-T1 disc (F_z) of the specimens were recorded. The specimens were preconditioned by loading and unloading at 2 Nm for three cycles to eliminate the viscoelastic

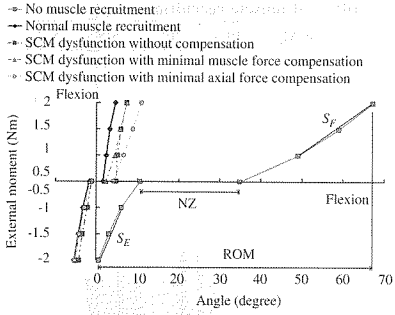

Fig. 3 The averaged load-displacement curve of spinal specimen. Positive angle and positive magnitude of moment indicate the flexion direction. NZ: neutral zone; ROM: range of motion; S_F: flexion stiffness; S_E: extension stiffness

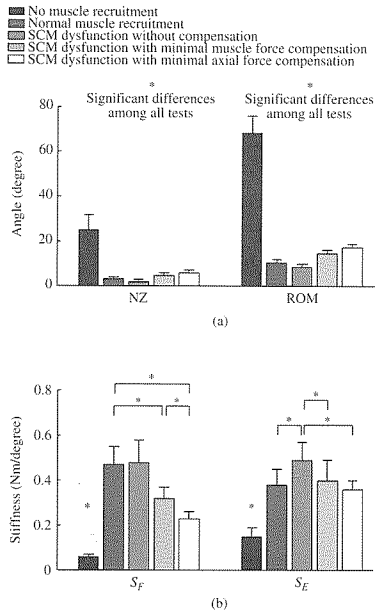

Fig. 4 The mean and standard deviation of: (a) the neutral zone (NZ) and range of motion (ROM), and (b) the flexion and extension stiffness (S_F, S_E) in different muscle conditions. *: $P < 0.05$

effects (Panjabi *et al.*, 2001). In the subsequent cycle, the specimens were loaded with stepwise pure moments from 0.5 Nm to 2 Nm increasingly in the flexion and then in the extension direction. The spinal stability in the sagittal plane was evaluated by the neutral zone (NZ) and the range of motion (ROM) (Panjabi *et al.*, 1989; Panjabi *et al.*, 2001). The NZ was defined as the sagittal angular displacement of spinal segments (C2-T1) at 0.5 Nm external flexion-extension bending moment. The ROM was defined as the sagittal angular displacement of spinal segments at 2 Nm external flexion-extension bending moment. The stiffness of the specimens during flexion and extension motion (S_F and S_E, Nm/°) were defined as the slope of load-displacement curve between 1 Nm and 2 Nm external moments. The initial position of the normal muscle recruitment test was assumed to be the neutral position. The θ_x, θ_y, θ_z were defined as the differences of initial positions between normal muscle recruitment test and other tests in sagittal, coronal, and axial planes respectively. Positive angles of θ_x, θ_y, θ_z mean the shifted positions from the neutral toward flexion, right lateral bending, and right axial rotation directions. The measurements of current study included the NZ, ROM, S_F, S_E, θ_x, θ_y, θ_z, and F_z. Analysis of variance (ANOVA) was used to examine the effect of different muscle conditions on these measurements. Multiple comparisons among the five test groups were also conducted. The significance level was set at 0.05.

III. RESULTS

The averaged load-displacement curve showed that the initial position of specimens without muscle recruitment was in flexion direction (14.8°) compared to the one with normal muscle recruitment. The flexion angle at 2 Nm external moments of no muscle recruitment specimen was up to 68° and the extension angle was close to 0° (Fig. 3). The NZ and ROM of no muscle recruitment specimen were 25.1° ± 6.8° and 68.5° ± 7.7°, respectively. The rotational stiffness of no muscle recruitment specimen of extension (S_E: 0.15 ± 0.04 Nm/°) was higher than the one of flexion (S_F: 0.06 ± 0.01 Nm/°). Compared to the no muscle recruitment test, the muscle recruitment tests showed significantly decreased NZ (1.8° ~ 5.9°) and ROM (8.4° ~ 17.4°), and increased flexion and extension stiffness (up to 0.49 Nm/°) of the specimens (all $P < 0.001$, Fig. 4 and Table 2).

The NZ and ROM were 3.2° ± 0.8° and 10.5° ± 1.3° in the normal muscle recruitment test. Considering the NZ and ROM of normal muscle recruitment as a base for comparison, the SCM dysfunction without compensation strategy decreased NZ and ROM to 1.8° ± 1.1° and 8.4° ± 1.6° ($P = 0.012$). However, the NZ and ROM of the two compensation tests were

Table 2 Mean ± standard deviation of all measurements in five muscle recruitment tests

	No muscle recruitment	Normal muscle recruitment	SCM dysfunction without compensation	SCM dysfunction with minimal muscle force compensation	SCM dysfunction with minimal axial force compensation
NZ (°)	25.1 ± 6.8	3.2 ± 0.8	1.8 ± 1.1	4.7 ± 1.1	5.9 ± 1.1
ROM (°)	68.5 ± 7.7	10.5 ± 1.3	8.4 ± 1.6	14.6 ± 1.7	17.4 ± 1.4
S_F (Nm/°)	0.06 ± 0.01	0.47 ± 0.08	0.48 ± 0.10	0.32 ± 0.05	0.23 ± 0.03
S_E (Nm/°)	0.15 ± 0.04	0.38 ± 0.07	0.49 ± 0.08	0.40 ± 0.09	0.36 ± 0.04
θ_x (°)	14.8 ± 0.8	–	-4.1 ± 1.2	-0.1 ± 0.7	-0.5 ± 1.0
θ_y (°)	0.6 ± 1.6	–	-7.2 ± 1.6	-0.6 ± 1.4	3.1 ± 1.5
θ_z (°)	0.6 ± 1.5	–	3.5 ± 0.7	0.1 ± 0.7	-0.7 ± 1.0
F_z (N)	–	78.0 ± 0.8	67.8 ± 0.9	43.0 ± 0.7	42.0 ± 0.6

NZ: neutral zone; ROM: range of motion; S_F: flexion stiffness; S_E: extension stiffness; θ_x, θ_y, θ_z: the differences of initial positions from those in normal muscle recruitment test in sagittal, coronal, and axial planes respectively; F_z: resultant axial force.

both significantly larger than the ones of normal muscle recruitment test (all $P < 0.01$). The NZ and ROM of SCM dysfunction with minimal axial force compensation test (5.9° ± 1.1° and 17.4° ± 1.4°) were larger than those with minimal muscle force compensation test (4.7° ± 1.1° and 14.6° ± 1.7°) (all $P < 0.05$, Fig. 4(a)).

The stiffness in SCM dysfunction without compensation test (S_F and S_E were 0.48 ± 0.10 Nm/° and 0.49 ± 0.08 Nm/° respectively) were significantly higher than the ones in other recruitment tests (all $P < 0.01$). The S_F of normal muscle recruitment test (0.47 ± 0.08 Nm/°) was larger than the one of SCM dysfunction with minimal muscle force compensation test (0.32 ± 0.05 Nm/°, $P < 0.001$) and with minimal axial force compensation test (0.23 ± 0.03 Nm/°, $P < 0.001$). The S_F of SCM dysfunction with minimal muscle force compensation test was also significantly larger than the one with minimal axial force compensation test ($P = 0.019$). There were no significant differences of S_E among the normal muscle recruitment test and the two compensation tests (0.36~0.40 Nm/°) (Fig. 4(b)).

Considering the initial position of normal muscle recruitment test as the neutral position, the initial position of no muscle recruitment showed large diversion toward flexion direction (θ_x: 14.8° ± 0.8°) while the diversion in coronal and axial plane were very small (around 0.6° ± 1.6°). In SCM dysfunction without compensation test, the initial position of specimen twisted toward extension (θ_x: -4.1° ± 1.2°), left lateral bending (θ_y: -7.2° ± 1.6°), and right axial rotation (θ_z: 3.5° ± 0.7°) directions. The differences of initial position in three planes (θ_x, θ_y, and θ_z) in SCM dysfunction without compensation test were all significantly larger than those in both the compensation tests (all $P < 0.001$). The differences of initial

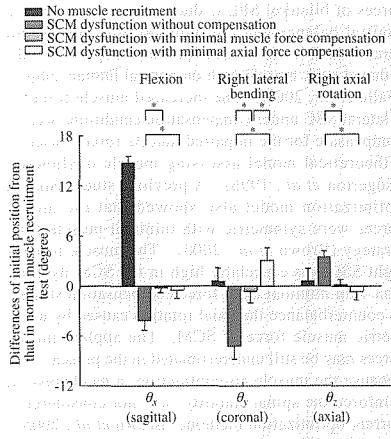

Fig. 5 The differences of the initial position from that in normal muscle recruitment test in sagittal, coronal, and axial planes (θ_x, θ_y, θ_z). Positive angles mean the flexion, right lateral bending, and right axial rotation directions. *: $P < 0.05$

position (θ_x, θ_y, and θ_z) were mostly smaller than 1° with muscle compensation strategies. There were no significant differences of initial positions between the two compensation tests except in coronal plane, i.e. θ_y was -0.6° ± 1.4° in SCM dysfunction with minimal muscle force compensation test and 3.1° ± 1.5° in SCM dysfunction with minimal axial force compensation test ($P = 0.001$, Fig. 5).

The normal muscle recruitment resulted in largest axial force (78.0 ± 0.8 N, $P < 0.001$). The axial force in SCM dysfunction without compensation test

(67.8 ± 0.9 N) was also larger than the axial force of the two compensation tests ($P < 0.001$). The axial force of SCM dysfunction test with minimal axial force compensation (42.0 ± 0.6 N) was smaller than the one with minimal muscle force compensation test (43.0 ± 0.7 N) ($P = 0.015$, Table 2).

IV. DISCUSSION

This study investigated the relationship between the stability of cervical spine and unilateral SCM dysfunction with different compensation strategies. Muscle strength decreases because of injury, fatigue, aging, and degeneration, but it does not reach zero (Mayer *et al.*, 1985). Thus the impaired SCM muscle force in this study was set to be about 1/4 of normal muscle force. The compensatory muscle forces illustrated in Table 1 were clinically observed or theoretically assumed. For example, the decreased muscle forces of bilateral SPL is due to the maintenance of sagittal balance and constant cervical contraction force, which is the result of previous experimentally-induced neck muscle pain on normal human subjects (Falla *et al.*, 2007). The increased muscle forces of bilateral SSC under compensation conditions were to compensate for the impaired muscle forces based on a theoretical model assessing muscle dysfunction (Edgerton *et al.*, 1996). A previous study using an optimization model also showed that the muscle forces were symmetric with minimal muscle force strategy (Brown *et al.*, 2005) . The muscle force of right SSC was especially high in the SCM dysfunction with minimal axial force compensation strategy to counterbalance the axial rotation caused by asymmetric muscle force of SCM. The applied muscle forces may be still underestimated in the present study because the muscle co-contraction, a mechanism to reinforce the spinal stability, was not considered in current optimization methods (Brown *et al.*, 2005).

The stiffness, ROM, and NZ of the specimen were generally used to quantify the intervertebral stability. The three parameters represented the rate, maximal, and minimal internal resistance opposed to the external load respectively. Segmental instability can be indexed by reduced stiffness or increased ROM and NZ. The bending stiffness was defined as the slope of the load-displacement curve (Wilke *et al.*, 1994). The ROM of the multi-segmental cervical spine was measured by given assumed maximal external pure moment from 1 Nm to 2.5 Nm (Panjabi *et al.*, 2001; Pitzen *et al.*, 2007; Wilke *et al.*, 1997). The NZ is commonly used to measure the displacement at which the resistance of movement is detected. Panjabi *et al.* (2001) defined the NZ as the angular rotation without external load to highlight the viscoelastic behavior. The definition of NZ in the current study was the angular rotation under fixed external load (i.e. 0.5 Nm) which provided larger but stable measurement (Zhao *et al.*, 2005).

Cautions should be used when interpreting the results. To simplify the study design, fixed sets of parameters, such as the muscle orientation, disc load, and muscle forces, were used without dealing with the geometric differences of specimens. Besides, those parameters were from the normal human model and were applied to all porcine specimens. This study was to determine the mechanism of how the muscle dysfunctions and compensations affect the cervical spine stability. Human cadaveric specimens were not used due to poor accessibility, uncontrolled bone quality due to age, and cost. This study showed that the length of the porcine cervical spines (C2-T1, 14.9 cm) was longer than the reported length of human cervical spine (C3-T1, 9.5 cm) (Kandziora *et al.*, 2001; Tan *et al.*, 2004). The average stiffness under flexion/extension external moments in this study was 0.11 ± 0.06 Nm/degree, and was 0.07 ± 0.02 Nm/degree in human specimens (C2-T2) (Ouyang *et al.*, 2005). The ROM of 2.0 Nm external load in this study was 68.5° and was close to the ROM of a human specimen (73.0°, C2-T1) (Wheeldon *et al.*, 2006). The NZ of the porcine cervical spine (25.1°) was, however, larger than the NZ of a human spine (14.0°, C2-C7) (Panjabi *et al.*, 2001). The specimen length and the shape of the facet joint between the porcine spine and human spine (Wang *et al.*, 2004; Yingling *et al.*, 1999) may be different. Nevertheless, the kinematic behaviors between human and porcine models without muscle recruitment may be considered comparable.

The SCM dysfunction without compensation test showed the smallest NZ and ROM. It should be noted that this test also showed large twisted initial positions in three planes (θ_x, θ_y, and θ_z). The bias position may constrain the spinal movement and show "locking" phenomena violating the clinical manifestations. This study suggested that the compensation strategy should be considered in the in vitro study when investigating unilateral muscle dysfunction.

There were significant increases of NZ and ROM in the two compensation tests compared to the ones in the normal muscle recruitment test. Thus the muscle dysfunction with compensation strategies would not provide efficient spinal stability as the normal muscle did. The NZ and ROM in SCM dysfunction with minimal muscle force compensation test were smaller, but the flexion stiffness (S_F) and axial force (F_z) were larger than the ones in SCM dysfunction with minimal axial force compensation test. The minimal muscle force compensation strategy was presumed to minimize the energy expenditure, while the minimal axial force compensation strategy was to minimize the compressive stress on the intervertebral

disc (Brown *et al.*, 2005). The minimization of muscle force was therefore suggested to be a more desirable compensation strategy over the minimization of axial force since it decreases the consumed energy, maintains better spinal stability, and only increases intradiscal load (F_z) a small amount.

A previous study demonstrated that the NZ, ROM, and bending stiffness are complementary expressions of stability, and are highly correlated with each other (Zhao *et al.*, 2005). In other words, the spinal stability in terms of stiffness corresponds to the observation from the NZ and ROM. However, the S_F in the current study was significantly different among the normal muscle recruitment test and the two compensation tests, but the S_E was not. This may be due to the extension stiffness which was constrained by strong neck flexors failing to reflect the subtle differences among different muscle recruitments. Thus the S_F could be a more sensitive index for examination of the stiffness of specimen with muscle recruitments.

The results of the present experiment indicated that muscle dysfunction affects the spinal stability. The study design focused on sub-acute muscle injury stage (i.e., the muscle spasm response subsides) with normal CNS control (capable of generating the "optimal" strategy). This study revealed an important clinical implication, that the cervical spine stability may not be sufficiently maintained in patients suffering cervical muscle dysfunction. If the impaired muscles are not treated properly (e.g. muscle re-education or strengthening exercises), the prolonged muscle dysfunction may induce permanent modification of CNS control pattern from altered neural input and changed muscle properties (Falla *et al.*, 2008). The abnormal control pattern would shift loads to the intervertebral discs and ligaments, decrease the role of the facet joint in transmitting load and stabilizing the spine (Goel *et al.*, 1993; Kong *et al.*, 1996), and then cause chronic pain eventually (Panjabi, 1992). Further study can include the pain-adaptation model in the chronic stage of muscle dysfunction (Lund *et al.*, 1991) to complement the understanding between the muscle dysfunction and the spinal stability.

V. CONCLUSIONS

This in vitro study showed that the simulation of muscle dysfunction without proper compensation strategy would result in twisted posture of the specimen and restricted spinal motion. Thus the investigation of the unilateral muscle dysfunction in the in vitro study should incorporate compensation strategies. The impaired muscle with surrounding muscle compensations could not efficiently stabilize the cervical spine as the normal muscles did. The optimal condition with minimal muscle forces was suggested to provide better spinal stability than that with minimal axial forces. The current study demonstrated the potential to incorporate the presumed CNS control strategies into the in vitro study. More complex muscle interactions and their effects on the different kinds of spinal injury can be studied in the future.

ACKNOWLEDGEMENT

National Health Research Institute, Taiwan (NHRI-EX96-9425EI).

REFERENCE

Andersen, J. H., Haahr, J. P., and Frost, P., 2007, "Risk Factors for More Severe Regional Musculoskeletal Symptoms: A Two-Year Prospective Study of a General Working Population," *Arthritis and Rheumatism*, Vol. 56, No. 4, pp. 1355-1364.

Arjmand, N., and Shirazi-Adl, A., 2006, "Sensitivity of Kinematics-Based Model Predictions to Optimization Criteria in Static Lifting Tasks," *Medical Engineering and Physics*, Vol. 28, No. 6, pp. 504-514.

Brown, S. H., and Potvin, J. R., 2005, "Constraining Spine Stability Levels in an Optimization Model Leads to the Prediction of Trunk Muscle Cocontraction and Improved Spine Compression Force Estimates," *Journal of Biomechanics*, Vol. 38, No. 4, pp. 745-754.

Buchanan, T. S., and Shreeve, D. A., 1996, "An Evaluation of Optimization Techniques for the Prediction of Muscle Activation Patterns During Isometric Tasks," *Journal of Biomechanical Engineering*, Vol. 118, No. 4, pp. 565-574.

Choi, H., and Vanderby, R. J., 1999, "Comparison of Biomechanical Human Neck Models: Muscle Forces and Spinal Loads at C4/5 Level," *Journal of Applied Biomechanics*, Vol. 15, No. 2, pp. 120-138.

Crisco, J. J., 3rd, and Panjabi, M. M., 1991, "The Intersegmental and Multisegmental Muscles of the Lumbar Spine. A Biomechanical Model Comparing Lateral Stabilizing Potential," *Spine*, Vol. 16, No. 7, pp. 793-799.

Edgerton, V. R., Wolf, S. L., Levendowski, D. J., and Roy, R. R., 1996, "Theoretical Basis for Patterning EMG Amplitudes to Assess Muscle Dysfunction," *Medicine and Science in Sports and Exercise*, Vol. 28, No. 6, pp. 744-751.

Essendrop, M., Andersen, T. B., and Schibye, B., 2002, "Increase in Spinal Stability Obtained at Levels of Intra-Abdominal Pressure and Back Muscle Activity Realistic to Work Situations,"

Applied Ergonomics, Vol. 33, No. 5, pp. 471-476.

Falla, D., Farina, D., Dahl, M. K., and Graven-Nielsen, T., 2007, "Muscle Pain Induces Task-Dependent Changes in Cervical Agonist/Antagonist Activity," *Journal of Applied Physiology*, Vol. 102, No. 2, pp. 601-609.

Falla, D., and Farina, D., 2008, "Neuromuscular Adaptation in Experimental and Clinical Neck Pain," *Journal of Electromyography and Kinesiology*, Vol. 18, No. 2, pp. 255-261.

Goel, V. K., Kong, W., Han, J. S., Weinstein, J. N., and Gilbertson, L. G., 1993, "A Combined Finite Element and Optimization Investigation of Lumbar Spine Mechanics with and without Muscles," *Spine*, Vol. 18, No. 11, pp. 1531-1541.

Hughes, R. E., Chaffin, D. B., Lavender, S. A., and Andersson, G. B., 1994, "Evaluation of Muscle Force Prediction Models of the Lumbar Trunk Using Surface Electromyography," *Journal of Orthopaedic Research*, Vol. 12, No. 5, pp. 689-698.

Kandziora, F., Pflugmacher, R., Scholz, M., Schnake, K., Lucke, M., Schroder, R., and Mittlmeier, T., 2001, "Comparison between Sheep and Human Cervical Spines: An Anatomic, Radiographic, Bone Mineral Density, and Biomechanical Study," *Spine*, Vol. 26, No. 9, pp. 1028-1037.

Kettler, A., Hartwig, E., Schultheiss, M., Claes, L., and Wilke, H. J., 2002, "Mechanically Simulated Muscle Forces Strongly Stabilize Intact and Injured Upper Cervical Spine Specimens," *Journal of Biomechanics*, Vol. 35, No. 3, pp. 339-346.

Kong, W. Z., Goel, V. K., Gilbertson, L. G., and Weinstein, J. N., 1996, "Effects of Muscle Dysfunction on Lumbar Spine Mechanics. A Finite Element Study Based on a Two Motion Segments Model," *Spine*, Vol. 21, No. 19, pp. 2197-2206; discussion 2206-2197.

Langenderfer, J., LaScalza, S., Mell, A., Carpenter, J. E., Kuhn, J. E., and Hughes, R. E., 2005, "An EMG-Driven Model of the Upper Extremity and Estimation of Long Head Biceps Force," *Computers in Biology and Medicine*, Vol. 35, No. 1, pp. 25-39.

Lee, P. J., Rogers, E. L., and Granata, K. P., 2006, "Active Trunk Stiffness Increases with Co-contraction," *Journal of Electromyography and Kinesiology*, Vol. 16, No. 1, pp. 51-57.

Lund, J. P., Donga, R., Widmer, C. G., and Stohler, C. S., 1991, "The Pain-Adaptation Model: A Discussion of the Relationship between Chronic Musculoskeletal Pain and Motor Activity," *Canadian Journal of Physiology and Pharmacology*, Vol. 69, No. 5, pp. 683-694.

Mayer, T. G., Smith, S. S., Keeley, J., and Mooney, V., 1985, "Quantification of Lumbar Function. Part 2: Sagittal Plane Trunk Strength in Chronic Low-Back Pain Patients," *Spine*, Vol. 10, No. 8, pp. 765-772.

Moroney, S. P., Schultz, A. B., and Miller, J. A., 1988, "Analysis and Measurement of Neck Loads," *Journal of Orthopaedic Research*, Vol. 6, No. 5, pp. 713-720.

Nachemson, A., 1985, "Lumbar Spine Instability. A Critical Update and Symposium Summary," *Spine*, Vol. 10, No. 3, pp. 290-291.

Ouyang, J., Zhu, Q., Zhao, W., Xu, Y., Chen, W., and Zhong, S., 2005, "Biomechanical Assessment of the Pediatric Cervical Spine under Bending and Tensile Loading," *Spine*, Vol. 30, No. 24, pp. E716-723.

Panjabi, M. M., Abumi, K., Duranceau, J., and Oxland, T., 1989, "Spinal Stability and Intersegmental Muscle Forces. A Biomechanical Model," *Spine*, Vol. 14, No. 2, pp. 194-200.

Panjabi, M. M., 1992, "The Stabilizing System of the Spine. Part I. Function, Dysfunction, Adaptation, and Enhancement," *Journal of Spinal Disorders*, Vol. 5, No. 4, pp. 383-389; discussion 397.

Panjabi, M. M., Crisco, J. J., Vasavada, A., Oda, T., Cholewicki, J., Nibu, K., and Shin, E., 2001, "Mechanical Properties of the Human Cervical Spine as Shown by Three-Dimensional Load-Displacement Curves," *Spine*, Vol. 26, No. 24, pp. 2692-2700.

Panjabi, M. M., 2007, "Hybrid Multidirectional Test Method to Evaluate Spinal Adjacent-Level Effects," *Clinical Biomechanics*, Vol. 22, No. 3, pp. 257-265.

Pitzen, T., Kettler, A., Drumm, J., Nabhan, A., Steudel, W. I., Claes, L., and Wilke, H. J., 2007, "Cervical Spine Disc Prosthesis: Radiographic, Biomechanical and Morphological Post Mortal Findings 12 Weeks after Implantation. A Retrieval Example," *European Spine Journal*, Vol. 16, No. 7, pp. 1015-1020.

Snijders, C. J., Hoek van Dijke, G. A., and Roosch, E. R., 1991, "A Biomechanical Model for the Analysis of the Cervical Spine in Static Postures," *Journal of Biomechanics*, Vol. 24, No. 9, pp. 783-792.

Tan, S. H., Teo, E. C., and Chua, H. C., 2004, "Quantitative Three-Dimensional Anatomy of Cervical, Thoracic and Lumbar Vertebrae of Chinese Singaporeans," *European Spine Journal*, Vol. 13, No. 2, pp. 137-146.

Vasavada, A. N., Li, S., and Delp, S. L., 1998, "Influence of Muscle Morphometry and Moment Arms on the Moment-Generating Capacity of Human Neck Muscles," *Spine*, Vol. 23, No. 4, pp. 412-422.

Wang, J. L., Tsai, Y. C., and Yang, B. D., 2004, "Strain Energy Density Distribution of Vertebral

Body of Two Motion Segment Model under Combined Compression and Sagiral Bending Momentan in Vitro Porcine Spine Biomechanical Study," *Journal of the Chinese Institute of Engineers*, Vol. 27, No. 6, pp. 927-934.

Wheeldon, J. A., Pintar, F. A., Knowles, S., and Yoganandan, N., 2006, "Experimental Flexion/Extension Data Corridors for Validation of Finite Element Models of the Young, Normal Cervical Spine," *Journal of Biomechanics*, Vol. 39, No. 2, pp. 375-380.

Wilke, H. J., Claes, L., Schmitt, H., and Wolf, S., 1994, "A Universal Spine Tester for in Vitro Experiments with Muscle Force Simulation," *European Spine Journal*, Vol. 3, No. 2, pp. 91-97.

Wilke, H. J., Wolf, S., Claes, L. E., Arand, M., and Wiesend, A., 1995, "Stability Increase of the Lumbar Spine with Different Muscle Groups. A Biomechanical in Vitro Study," *Spine*, Vol. 20, No. 2, pp. 192-198.

Wilke, H. J., Kettler, A., and Claes, L. E., 1997, "Are Sheep Spines a Valid Biomechanical Model for Human Spines?," *Spine*, Vol. 22, No. 20, pp. 2365-2374.

Yingling, V. R., Callaghan, J. P., and McGill, S. M., 1999, "The Porcine Cervical Spine as a Model of the Human Lumbar Spine: An Anatomical, Geometric, and Functional Comparison," *Journal of Spinal Disorders*, Vol. 12, No. 5, pp. 415-423.

Zhao, F., Pollintine, P., Hole, B. D., Dolan, P., and Adams, M. A., 2005, "Discogenic Origins of Spinal Instability," *Spine*, Vol. 30, No. 23, pp. 2621-2630.

Manuscript Received: Oct. 04, 2007
Revision Received: Feb. 19, 2008
and Accepted: Mar. 19, 2008